Translocation of calmodulin to the nucleus supports CREB phosphorylation in hippocampal neurons

Karl Deisseroth*, E. Kevin Heist† & Richard W. Tsien*

** Department of Molecular and Cellular Physiology, Beckman Center for Molecular and Genetic Medicine, and †Department of Neurobiology, Stanford University School of Medicine, Stanford, California 94305-5426, USA*

Activation of the transcription factor CREB is thought to be important in the formation of long-term memory in several animal species[1–3]. The phosphorylation of a serine residue at position 133 of CREB is critical for activation of CREB[4]. This phosphorylation is rapid when driven by brief synaptic activity in hippocampal neurons[5]. It is initiated by a highly local, rise in calcium ion concentration[5] near the cell membrane, but culminates in the activation of a specific calmodulin-dependent kinase known as CaMK IV (ref. 7), which is constitutively present in the neuronal nucleus[7,8]. It is unclear how the signal is conveyed from the synapse to the nucleus. We show here that brief bursts of activity cause a swift (~1 min) translocation of calmodulin from the cytoplasm to the nucleus, and that this translocation is important for the rapid phosphorylation of CREB. Certain Ca^{2+} entry systems (L-type Ca^{2+} channels and NMDA receptors) are able to cause mobilization of calmodulin, whereas others (N- and P/Q-type Ca^{2+} channels) are not. This translocation of calmodulin provides a form of cellular communication that combines the specificity of local Ca^{2+} signalling with the ability to produce action at a distance.

In hippocampal neurons subjected to synaptic stimulation or direct depolarization, Ca^{2+}-dependent CREB phosphorylation occurs even when elevation in bulk $[Ca^{2+}]_i$ has been suppressed with internal EGTA[5], suggesting that the signalling from synapse to nucleus does not involve the spread of free Ca^{2+} *per se*. We looked instead for translocation of a Ca^{2+} effector. Examination of an array of calmodulin (CaM) kinases[9,10] in CA3/CA1 hippocampal pyramidal neurons, including CaMKI, CaMKIIα, CaMKIIβ, CaMKIV and CaMKKα, failed to reveal any striking redistribution upon strong direct depolarization of the neurons (for 180 s in 90 mM K^+) (Fig. 1a). Although calmodulin itself is largely immobile in quiescent cells[11], changes in its localization to various cellular compartments, including to the nucleus, have been described[11–13]. We therefore investigated whether the CaM translocation could be rapid enough to account for signalling on a timescale of minutes.

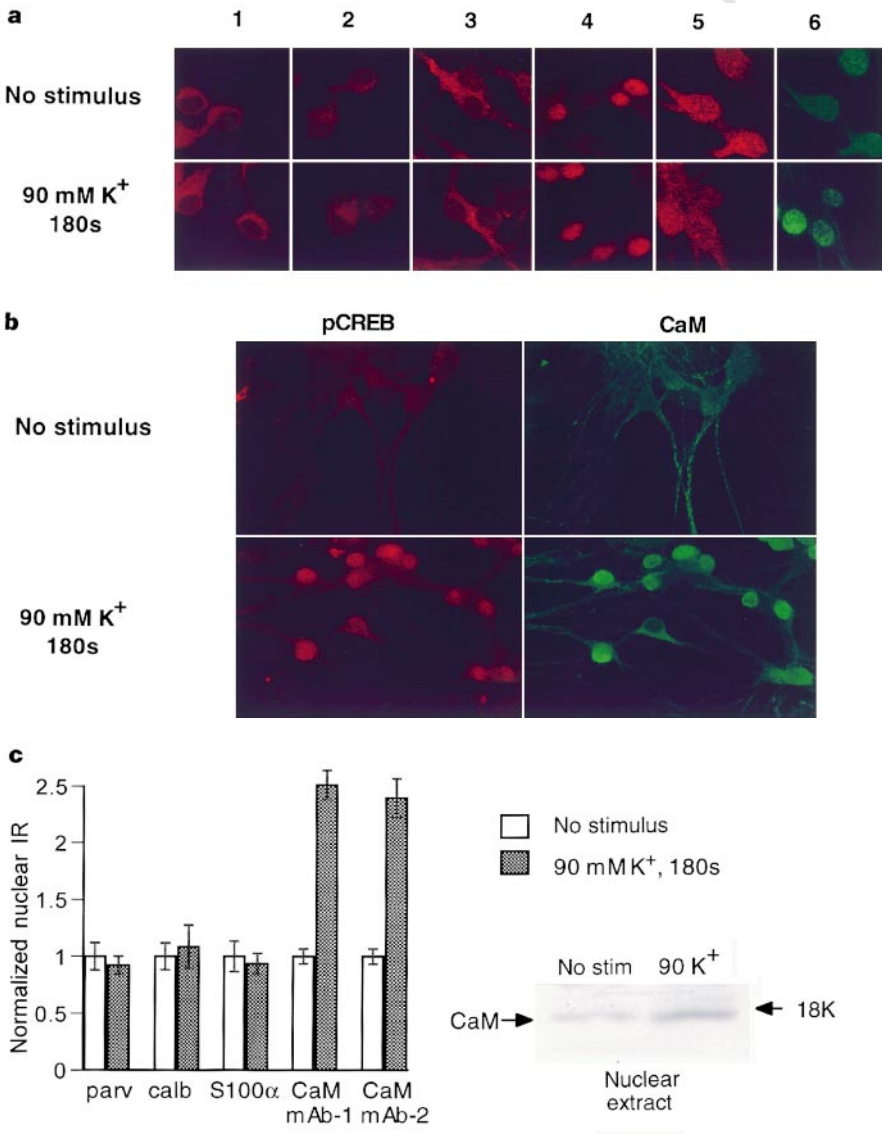

Figure 1 Rapid activity-dependent translocation of calmodulin to the nucleus in hippocampal CA3/CA1 pyramidal neurons. **a**, Confocal mid-nuclear sections showing CaMKI (1), CaMKIIα (2), CaMKIIβ (3), CaMKIV (4), CaMKKα (5), and CaM (6) immunofluorescence with or without stimulation. The same field of cells is shown in panels 5 and 6. **b**, Dendritic/nuclear confocal sections showing CaM translocation and CREB phosphorylation as a result of depolarization. **c**, Quantification of nuclear confocal data on CaM and other Ca^{2+}-binding proteins. No activity-dependent redistribution to the nucleus was observed for parvalbumin, calbindin D28K, or S100α ($n > 50$ neurons; $P > 0.2$, error bars signify ±1 s.e.m.). pCREB immunoreactivity was found to be increased in the same neurons, verifying that they had been successfully stimulated. In contrast, the 6D4 anti-CaM (mAb-2) revealed an increase in nuclear CaM, similar to results obtained with the UBI antibody (mAb-1) ($P < 0.001$ in both cases). Inset, nuclear extracts from stimulated cells showed increased CaM content (2.4-fold), as assessed by immunoblot.

We found a rapid, activity-dependent increase in CaM immunoreactivity (CaM-IR) in the nucleus by using a monoclonal antibody that recognizes CaM regardless of whether it is associated with Ca^{2+} (ref. 29) or a target kinase[14] (Fig. 1a). Nuclear CaM was readily detectable without stimulation, but increased strongly after stimulation. The CaM-IR (Fig. 1a, mid-nuclear sections; Fig. 1b, right, dendritic/nuclear sections) appeared to be closely correlated with nuclear CREB phosphorylation (Fig. 1b, left). Similar results were obtained within 42 s of applying briefer stimuli (18 s of 50 Hz electrical field stimulation, Fig. 2; or 18 s of 90 mM K^+, not shown). Comparable increases in nuclear CaM-IR were found with a second monoclonal antibody (mAb-2; Fig. 1c). In contrast, no redistribution was seen for other Ca^{2+}-binding proteins, parvalbumin, calbindin D28K, and S100α, in neurons expressing these markers (Fig. 1c). A parallel activity-dependent reduction in cytosolic CaM-IR was measured at the apical dendrite (52% ± 9% of control, $P < 0.01$). CaM translocation slowly reversed on a timescale of tens of minutes after stimulation (Fig. 4c). We confirmed the increase of nuclear CaM by subcellular fractionation. Depolarization (180 s of 90 mM K^+) caused a sizeable increase (2.4-fold) in nuclear CaM (Fig. 1c, inset). In a third approach, we tracked CaM translocation using a merocyanine-labelled calmodulin, MeroCaM[15], introduced into individual neurons by patch pipette. Rapid (~1 min) elevations in nuclear MeroCaM were observed upon depolarization, whereas opposite changes in MeroCaM fluorescence were observed in cytoplasm, consistent with a net translocation (not shown); in addition, ratiometric imaging (F_{605}/F_{530}) demonstrated a rapid (~1 min) increase in the nuclear ratio of Ca^{2+}/MeroCaM to apo-MeroCaM, indicating that the proportion of nuclear CaM in the Ca^{2+}-bound state was also increased by membrane depolarization.

Brief bursts of electrical stimulation (50 Hz for 18 s) also gave rise to a marked translocation of CaM to the nucleus (Fig. 2a, b), which was sharply diminished by the L-type Ca^{2+}-channel antagonist nimodipine (10 μM). The stimulus-induced rise in nuclear CaM-IR was also blunted by the NMDA-receptor antagonist D-AP5 (50 μM) and was eliminated completely when D-AP5 and nimodipine were applied together, whereas maximal blockade of N-type Ca^{2+} channels by ω-CTx GVIA (1 μM) barely reduced CaM. This latter effect could be due to the inhibition of presynaptic N-type channels contributing to synaptic glutamate release. To focus on the postsynaptic N-type channels, we bypassed the presynaptic terminal by imposing direct depolarization (90 mM K^+) in the presence of AP5 (Fig. 2c, d). In this case, ω-CTx GVIA did not reduce CaM translocation. Likewise, blockade of postsynaptic P/Q-type channels with saturating ω-AgaIVA (1 μM) was ineffective, whereas nimodipine blocked CaM translocation (Fig. 2d). We compared the contributions of the various channel types[6,16,17] to depolarization-induced rises in somatic intracellular calcium ion concentration ($[Ca^{2+}]_i$) (Fig. 2d) under the conditions used to study CaM translocation (Fig. 2c). The contribution of L-type channels was significantly less than that of P/Q-type channels at every time point, and less than that of N-type channels at the time of peak $[Ca^{2+}]_i$, although the L-type channels contributed more to the plateau of $[Ca^{2+}]_i$ than did the N-type channels. Thus, CaM translocation cannot result simply from a bulk increase in $[Ca^{2+}]_i$, suggesting that coupling could be more specific between L-type channel activity and CaM or CaM-binding proteins.

If CaM translocation is necessary for signalling to the nucleus, the requirements for Ca^{2+} entry that apply to initiation of CaM translocation should also extend to the downstream nuclear event. Although L-type Ca^{2+} channels have long been implicated in gene expression[18,19], the importance of N- or P/Q-type channels has not

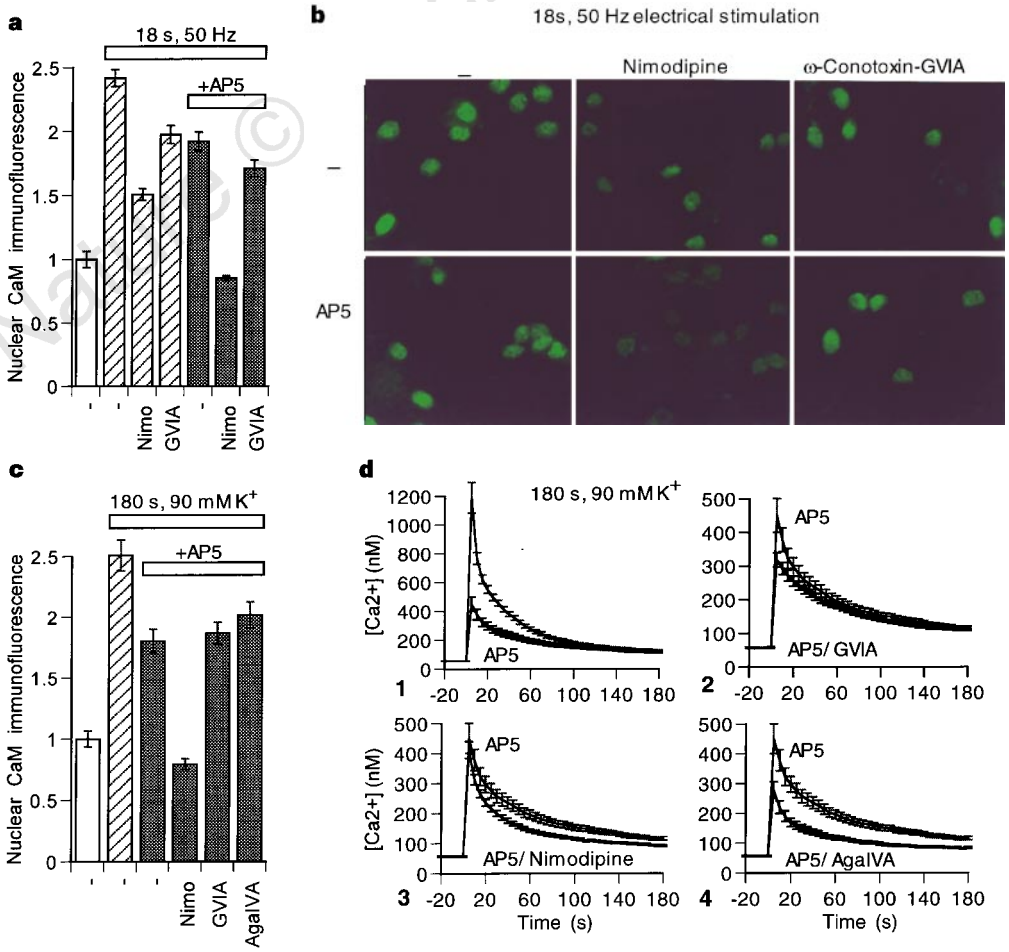

Figure 2 Selective control of activity-dependent CaM translocation by NMDA receptors and L-type Ca^{2+} channels. **a**, Effects of Ca^{2+} influx inhibitors on CaM translocation to the nucleus following brief electrical stimulation. All antagonist effects were highly significant ($P < 0.001$, $n > 50$ cells for each condition). **b**, Representative confocal sections used for analysis in **a**. **c**, Effects of Ca^{2+} influx inhibitors on CaM translocation to the nucleus following stimulation with 90 mM K^+ (3 min). In the presence of D-AP5, the nimodipine effect was highly significant ($P < 0.001$), whereas the effects of GVIA or AgaIVA were not ($P > 0.2$). **d**, Intracellular free $[Ca^{2+}]$ at the cell body measured with Fura-2 during depolarization under the conditions of **c**. D-AP5 strongly reduced the 90 mM K^+-induced Ca^{2+} transient (1). Reduction of the somatic Ca^{2+} signal in D-AP5 by the Ca^{2+} channel antagonists ω-conotoxin GVIA (2), nimodipine (3), or ω-AgaIVA (4). The effect of ω-conotoxin GVIA was greater than the effect of nimodipine over the first 15 s of stimulation, but not beyond this point. The effect of AgaIVA was significantly greater than the effect of nimodipine throughout ($P < 0.001$ at the beginning, $P < 0.05$ at the end).

been systematically examined. We found a pharmacological profile for CREB Ser 133 phosphorylation[20] (Fig. 3a, b) very similar to that of CaM mobilization (Fig. 2a–c). Blockade of P/Q- or N-type channels was completely ineffective in reducing CREB phosphorylation (Fig. 3b), despite their strong participation in triggering an increase in $[Ca^{2+}]_i$ (Fig. 2d). The privileged linkage between L-type Ca^{2+} entry and CaM translocation to the nucleus thus extends to the putative outcome of the translocation.

To test the importance of nuclear CaM in synaptically induced CREB phosphorylation, we compared the immunoreactivities of CaM-IR and Ser 133-pCREB-IR in individual nuclei across a large population of cells. There was a strong correlation between levels of nuclear CaM and nuclear pCREB after 50 Hz electrical stimulation (Fig. 3c, $r = 0.907$, $n = 201$, $P < 0.0001$; Fig. 1b). The relation was maintained under partial pharmacological inhibition (Fig. 3d): the greater the reduction in nuclear CaM, the greater the decrease in pCREB. Like the results of Ca^{2+}-channel blockade, our results support the idea that nuclear CaM could be limiting in rapid CaM-kinase-dependent CREB phosphorylation. In contrast, stimulation of cyclic-AMP signalling with forskolin increased pCREB, weakly at 5 min and strongly at 30 min, but with no clear correlation with changes in nuclear CaM (Figs 3d, 4d). Presumably, forskolin promotes CREB phosphorylation through translocation of protein kinase A to the nucleus[21,22] and not through the CaM translocation and CaM kinase mechanism recruited by synaptic activity. The efficacy of CaM translocation as triggered by Ca^{2+} influx through L-type channels was demonstrated by using a direct activator of L-type channel activity, FPL 64176 (Fig. 3e). When applied for 3 min, this agent increased nuclear CaM-IR several-fold, again with strongly correlated increases in nuclear pCREB. Previous work has shown a substantial increase in nuclear calmodulin after 1 h of Bay K8644 treatment *in vivo*[13].

To interfere with CaM import into the nucleus, we exploited the extreme temperature-sensitivity[12] of this process (diffusive processes such as entry of the protein kinase A catalytic subunit into the nucleus are only slightly temperature-sensitive[22]). Moderate chilling after a brief burst of electrical activity (Fig. 4a) essentially abolished rapid translocation of CaM, although a slow leakage of CaM into the nucleus persisted at long times after the stimulus. This indicates that the nuclear translocation of CaM is not simply diffusive but may be facilitated[12], perhaps involving the cytoskeleton. Like CaM translocation, activity-dependent CREB phosphorylation is also sharply reduced by chilling, giving only a late increase at the lowered temperature (Fig. 4b). In contrast to behaviour triggered by synaptic activity, forskolin-stimulated CREB phosphorylation is not slowed by chilling[22] (Fig. 4d). No significant CaM translocation was observed with forskolin treatment, regardless of temperature (Fig. 4d). Reversal of CaM translocation reached baseline levels 2 h after stimulation (Fig. 4c).

To intercept CaM in the nucleus, we transfected hippocampal neurons[23] with a CaM-inhibitor peptide specifically targeted to the nucleus[24] (nCaMBP) (Fig. 5). The peptide's nuclear location was confirmed by staining with an nCaMBP-specific antibody[24] and counterstaining with DAPI (Fig. 5a). Depolarization with 20 mM K^+ produced a clear increase in pCREB that was abolished by nCaMBP (Fig. 5b, middle) but not in control transfected cells (Fig. 5b, left). When the strength of the depolarizing stimulus was increased, nCaMBP only partly reduced the increase in pCREB (Fig. 5b, c), consistent with the competitive mechanism of nCaMBP action[24] or perhaps with recruitment of an additional pathway by this very strong stimulus.

Our experiments have revealed a rapid, activity-dependent nuclear translocation of calmodulin and demonstrated its importance for neuronal CREB phosphorylation. The time course of CaM translocation is fast enough (~1–2 min) to account for the kinetics of nuclear CREB phosphorylation under similar conditions[5,7].

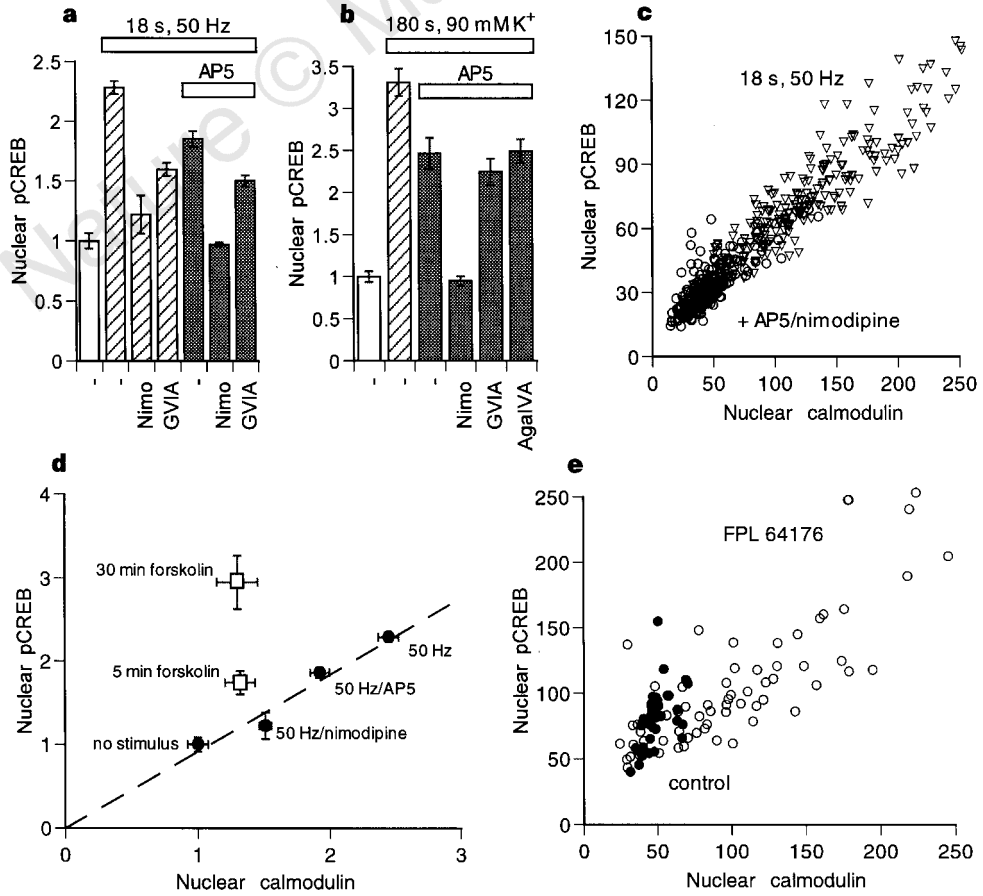

Figure 3 Close relationship between activity-dependent CaM translocation and CREB phosphorylation. **a**, Confocal quantification of CREB phosphorylation after synaptic stimulation at 50 Hz for 18 s. Experimental conditions and inhibitor concentrations as in Fig. 2a. All effects were highly significant relative to control ($P < 0.001$). **b**, Confocal quantification of CREB phosphorylation after 90 mM K^+ stimulation. The effects of D-AP5 alone and of nimodipine in D-AP5 were highly significant ($P < 0.001$), whereas the effects of ω-CTx-GVIA and ω-Aga-IVA in D-AP5 were not ($P > 0.2$). **c**, Single-cell correlation between CaM translocation and activity-dependent CREB phosphorylation, in response to 50 Hz electrical stimulation for 18 s (triangles, $n = 201$ cells, $r = 0.907$, $P < 0.0001$). Addition of D-AP5 and nimodipine (circles) reduced nuclear CaM and pCREB in parallel. **d**, Summary plot of mean values of CaM translocation and CREB phosphorylation under various stimulation conditions. **e**, FPL 64176 (5 μM) was applied in external solution containing TTX, D-AP5, ω-conotoxin GVIA, ω-AgaIVA, and CNQX (open symbols) and compared with sham controls (filled symbols).

Indeed, the arrival of CaM at the nucleus is critical for promoting CREB phosphorylation, as indicated by the insufficiency of basal nuclear CaM (Figs 2c, d, 3b), by the correlation between increased nuclear CaM and pCREB (Fig. 3), and by the effects on pCREB of blocking nuclear CaM import (Fig. 4) or of intercepting CaM in the nucleus (Fig. 5). Reinforcing the idea that signalling to the nucleus may originate from changes in local rather than in bulk $[Ca^{2+}]_i$ (refs 5, 25), even large increases in bulk $[Ca^{2+}]_i$ fail to promote CREB phosphorylation if not coupled with CaM translocation (Figs 2c, d, 3b). In fact, Ca^{2+} ions coming in may only need to reach apo-CaM near the plasma membrane to transmit the signal; molecules with a selective affinity for Ca^{2+}/CaM could be involved in CaM movement in the cell and would be expected to stabilize the Ca^{2+}-bound state. One nuclear target could be CaMKIV (refs 26, 27), which has been localized to the nucleus of hippocampal neurons and implicated in neuronal activity-dependent CREB phosphorylation[7]. CaMKIV can be phosphorylated and thereby activated by similarly CaM-dependent[28] kinase kinases. An isoform of CaMKK might translocate together with CaM, stabilizing Ca^{2+}-bound CaM and increasing the activity of CaMKIV. The exceptionally fast kinetics of this pathway activated by bursts of synaptic activity may be well suited for communication of rapid information from synapse to nucleus. □

Methods

Electrophysiology. CA3/CA1 hippocampal neurons were cultured essentially as described[5]. Synaptic activity was controlled by field electrical stimulation[5]; unlike high-K^+ depolarization, action potentials provided by the field electrodes are not sufficient when postsynaptic receptors are blocked to give rise to CREB phosphorylation, probably because fast action potentials are too brief to open slowly-activating L-type channels sufficiently. Neurons were preincubated for 2–3 h before stimulation in 1 μM tetrodotoxin (TTX) (Calbiochem); TTX was removed just before stimulation. Pharmacological agents were ω-agatoxin IVA and ω-conotoxin GVIA (Peptide Institute or Pfizer); nimodipine, D-AP5, FPL 64176, CNQX and forskolin (RBI).

Imaging. Imaging of Ca^{2+} and MeroCaM was done using a Videoscope ICCD camera. For Fura-2 Ca^{2+} imaging, data were taken from a measurement region encompassing the entire soma, including the nucleus. Neurons were fixed in

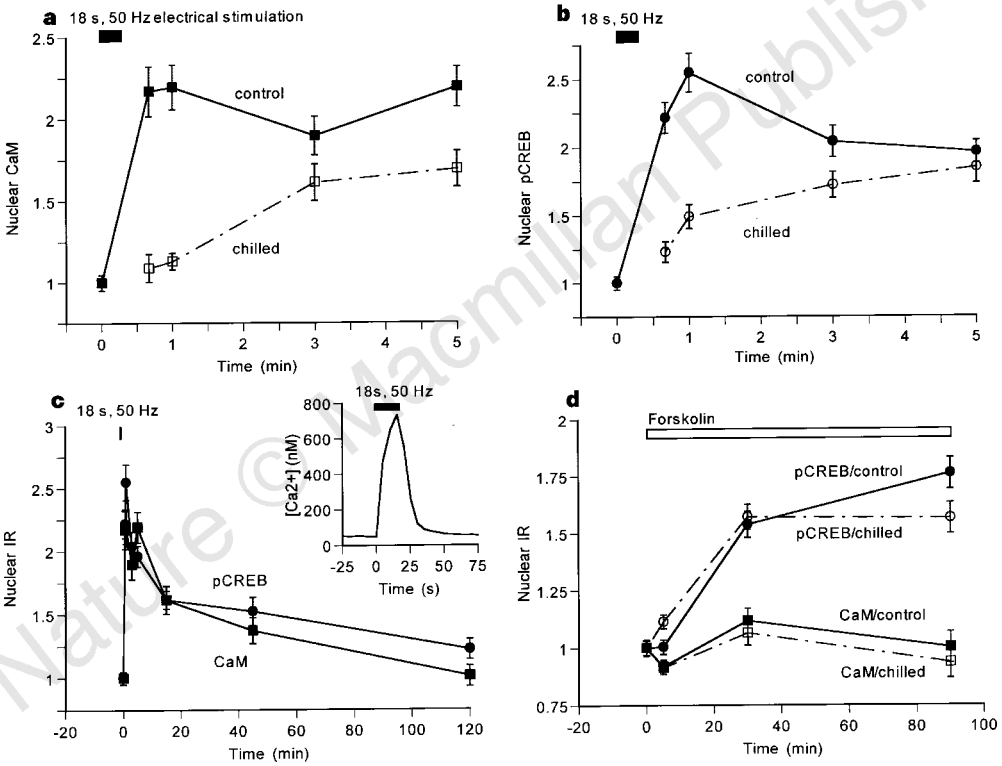

Figure 4 Requirement for nuclear CaM translocation in activity-dependent CREB phosphorylation. **a**, Post-stimulus chilling inhibits activity-dependent CaM translocation; this inhibition can be overcome at long times after the stimulus. **b**, Parallel inhibition of CREB phosphorylation under the same conditions. **c**, Time course of reversal of CaM translocation after cessation of brief electrical stimulation. Inset, time course of intracellular free $[Ca^{2+}]$ elevation in response to the stimulation (averaged trace, $n = 13$). **d**, cAMP-dependent CREB phosphorylation is not slowed by chilling.

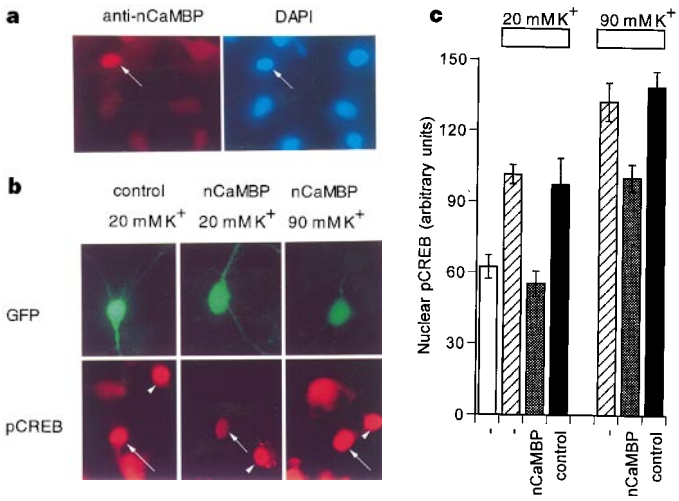

Figure 5 Causal link between nuclear CaM and activity-dependent CREB phosphorylation in hippocampal neurons. **a**, Nuclear localization of the transfected nuclear CaM binding protein (nCaMBP). DAPI stain (right) for DNA labels nuclei. **b**, Inhibition of activity-dependent (20 mM K^+) CREB phosphorylation by expression of nCaMBP (centre) but not in control transfection (left). Depolarization with 90 mM K^+ (right) was able largely to overcome the effect of nCaMBP. Arrows indicate transfected neurons identified by GFP fluorescence (GFP signal shown in upper row); arrowheads indicate non-transfected neurons nearby. Expression of nCaMBP did not affect neuronal morphology or total CREB levels (CREB immunofluorescence, 105.2 ± 14.5% of control, $n = 8$). **c**, nCaMBP abolished 20 mM K^+-induced CREB phosphorylation ($P < 0.01$, $n = 9$); empty vector had no effect ($P > 0.2$, $n = 14$). As a separate control, we coexpressed β-galactosidase instead of nCaMBP; no effect was seen on CREB phosphorylation (pCREB-IR 101.4 ± 11.2% relative to control, $n = 7$). nCaMBP partially inhibited 90 mM K^+-induced CREB phosphorylation ($P < 0.05$, $n = 16$), whereas transfection with empty vector did not ($P > 0.2$, $n = 13$).

ice-cold 4 mM EGTA/4% formaldehyde/PBS and permeabilized in 0.4% saponin or 0.1% Triton X-100 (fainter background staining was detected with saponin). The monoclonal anti-CaM antibodies (mAb-1 from UBI was used for all experiments except for Fig. 1c, for which mAb-2 from Sigma was also used) each recognize both Ca^{2+}-bound and Ca^{2+}-free forms of CaM[29,30]; the UBI antibody has a slight preference for Ca^{2+}-free CaM and the Sigma antibody Ca^{2+}-bound CaM; as all the fixations were in 4 mM EGTA, the antibodies gave quantitatively indistinguishable results (Fig. 1c). Other primary antibodies used were anti-calbindin D28K, anti-parvalbumin and anti-S100α (Sigma), anti-pCREB and anti-CREB (UBI), anti-CaMKI (gift from A. Nairn), anti-CaMKIIα and anti-CaMKIIβ (Life Technologies), anti-CaMKIV and anti-CaMKKα (Santa Cruz Biotechnology), and anti-nCaMBP (gift from M. Kaetzel and J. Dedman). For chilling experiments, cells were bathed at 7.5 °C or 24 °C within 5 s of electrical stimulation. Confocal sections were mid-nuclear; DAPI (4,6-diamidino-2-phenylindole) was used to validate the morphological identification of nuclei.

Transfection. Calcium phosphate transfections of neurons[23] were carried out in 24-well plates using 4 μg DNA per well. Neurons were exposed to the precipitate for 2 h in serum-free Optimem (GIBCO/BRL) and subsequently returned to normal culture medium for 48 h. In co-transfections, the green fluorescent protein (GFP) marker plasmid was put at a disadvantage to ensure that GFP-positive cells express the cotransfected plasmid, as verified by double-marker experiments. The E-GFP expression vector (pEGFP-C1) was from Clontech; other materials were gifts from J. Wang, M. Kaetzel and J. Dedman and have been described[24].

Subcellular fractionation. Fractionation was done essentially as described[5]: to hypotonic lysis buffer were added 2 mM $CaCl_2$, 1 mM $MgCl_2$, 1 mini-protease inhibitor tablet (Boehringer), and 2.5 mg ml^{-1} wheat germ agglutinin (WGA, Sigma; this WGA fraction exhibited some nonspecific binding to antibodies on western blot). Fractionation was carried out as near to 0 °C as possible. Protein concentrations were determined by the Bradford method, and 4 μg of each sample was loaded onto each lane for denaturing 15% SDS–PAGE and then transferred to nitrocellulose. The membrane was probed with anti-CaM monoclonal antibody (UBI) and detected by ECL.

Received 15 September; accepted 26 November 1997.

1. Dash, P. K., Hochner, B. & Kandel, E. R. Injection of the cAMP-responsive element into the nucleus of *Aplysia* sensory neurons blocks long-term facilitation. *Nature* **345,** 718–721 (1990).
2. Bourtchuladze, R. *et al.* Deficient long-term memory in mice with a targeted mutation of the cAMP-responsive element-binding protein. *Cell* **79,** 59–68 (1994).
3. Yin, J. C. *et al.* Induction of a dominant negative CREB transgene specifically blocks long-term memory in *Drosophila*. *Cell* **79,** 49–58 (1994).
4. Gonzalez, G. A. & Montminy, M. R. Cyclic AMP stimulates somatostatin gene transcription by phosphorylation of CREB at serine 133. *Cell* **59,** 675–680 (1989).
5. Deisscroth, K., Bito, H. & Tsien, R. W. Signaling from synapse to nucleus: postsynaptic CREB phosphorylation during multiple forms of hippocampal synaptic plasticity. *Neuron* **16,** 89–101 (1996).
6. Kavalali, E., Zhuo, M., Bito, H. & Tsien, R. W. Dendritic Ca2+ channels characterized by recordings from isolated hippocampal dendritic segments. *Neuron* **18,** 651–663 (1997).
7. Bito, H., Deisseroth, K. & Tsien, R. W. CREB phosphorylation and dephosphorylation: a Ca^{2+}- and stimulus duration-dependent switch for hippocampal gene expression. *Cell* **87,** 1203–1214 (1996).
8. Nakamura, Y., Okuno, S., Sato, F. & Fujisawa, H. An immunohistochemical study of Ca^{2+}/calmodulin-dependent protein kinase IV in the rat central nervous system: light and electron microscopic observations. *Neuroscience* **68,** 181–194 (1995).
9. Sheng, M., Thompson, M. A. & Greenberg, M. E. CREB: a Ca^{2+}-regulated transcription factor phosphorylated by calmodulin-dependent kinases. *Science* **252,** 1427–1430 (1991).
10. Dash, P. K., Karl, K. A., Colicos, M. A., Prywes, R. & Kandel, E. R. cAMP response element-binding protein is activated by Ca^{2+}/calmodulin- as well as cAMP-dependent protein kinase. *Proc. Natl Acad. Sci. USA* **88,** 5061–5065 (1991).
11. Luby-Phelps, K., Hori, M., Phelps, J. M. & Won, D. Ca^{2+}-regulated dynamic compartmentalization of calmodulin in living smooth muscle cells. *J. Biol. Chem.* **270,** 21532–21538 (1995).
12. Pruschy, M., Ju, Y., Spitz, L., Carafoli, E. & Goldfarb, D. S. Facilitated nuclear transport of calmodulin in tissue culture cells. *J. Cell Biol.* **127,** 1527–1536 (1994).
13. Vendrell, M., Pujol, M. J., Tusell, J. M. & Serratosa, J. Effect of different convulsants on calmodulin levels and proto-oncogene *c-fos* expression in the central nervous system. *Brain Res. Mol. Brain Res.* **14,** 285–292 (1992).
14. Mitsui, K., Brady, M., Palfrey, H. C. Nairn, A. C. Purification and characterization of calmodulin-dependent protein kinase III from rabbit reticulocytes and rat pancreas. *J. Biol. Chem.* **268,** 13422–13433 (1993).
15. Hahn, K. W., Waggoner, A. S. & Taylor, D. L. A calcium-sensitive fluorescent analog of calmodulin based on a novel calmodulin-binding fluorophore. *J. Biol. Chem.* **265,** 20335–20345 (1990).
16. Westenbroek, R. E., Ahlijanian, M. K. & Catterall, W. A. Clustering of L-type Ca^{2+} channels at the base of major dendrites in hippocampal pyramidal neurons. *Nature* **347,** 281–284 (1990).
17. Magee, J. C. & Johnston, D. Characterization of single voltage-gated Na^{2+} and Ca^{2+} channels in apical dendrites of rat CA1 pyramidal neurons. *J. Physiol.* **487,** 67–90 (1995).
18. Morgan, J. I. & Curran, T. Role of ion flux in the control of c-fos expression. *Nature* **322,** 552–555 (1986).
19. Murphy, T. H., Worley, P. F. & Barahan, J. M. L-type voltage-sensitive calcium channels mediate synaptic activation of immediate early genes. *Neuron* **7,** 625–635 (1991).
20. Ginty, D. D. *et al.* Regulation of CREB phosphorylation in the suprachiasmatic nucleus by light and a circadian clock. *Science* **260,** 238–241 (1993).
21. Hagiwara, M. *et al.* Coupling of hormonal stimulation and transcription via the cyclic AMP responsive factor CREB is rate limited by nuclear entry of protein kinase A. *Mol. Cell. Biol.* **13,** 4852–4859 (1993).
22. Harootunian, A. T. *et al.* Movement of the free catalytic subunit of cAMP-dependent protein kinase into and out of the nucleus can be explained by diffusion. *Mol. Biol. Cell.* **4,** 993–1002 (1993).
23. Xia, Z., Dudek, H., Miranti, C. K. & Greenberg, M. E. Calcium influx via the NMDA receptor induces immediate early gene transcription by a MAP kinase/ERK-dependent mechanism. *J. Neurosci.* **16,** 5425–5436 (1996).
24. Wang, J., Campos, B., Jamieson, G. A. Jr, Kaetzel, M. A. & Dedman, J. R. Functional elimination of calmodulin within the nucleus by targeted expression of an inhibitor peptide. *J. Biol. Chem.* **270,** 30245–30248 (1995).
25. Hardingham, G. E., Chawla, S., Johnson, C. M. & Bading, H. Distinct functions of nuclear and cytoplasmic calcium in the control of gene expression. *Nature* **385,** 260–265 (1997).
26. Means, A. R. *et al.* A novel Ca^{2+}/calmodulin-dependent protein kinase and a male germ cell-specific calmodulin-binding protein are derived from the same gene. *Mol. Cell. Biol.* **11,** 3960–3971 (1991).
27. Bito, H., Deisseroth, K. & Tsien, R. W. Ca^{2+}-dependent regulation in neuronal gene expression. *Curr. Opin. Neurobiol.* **7,** 419–429 (1997).
28. Tokumitsu, H. & Soderling, T. R. Requirements for calcium and calmodulin in the calmodulin kinase activation cascade. *J. Biol. Chem.* **271,** 5617–5622 (1996).
29. Sacks, D. B., Porter, S. E., Ladenson, J. H. & McDonald, J. M. Monoclonal antibody to calmodulin: development, characterization, and comparison with polyclonal anti-calmodulin antibodies. *Analyt. Biochem.* **194,** 369–377 (1991).
30. Hulen, D., Baron, A., Salisbury, J. & Clarke, M. Production and specificity of monoclonal antibodies against calmodulin from *Dicytostelium discoideum*. *Cell. Motil. Cytoskel.* **18,** 113–122 (1991).

Acknowledgements. We thank A. Nairn for antibodies; J. Dedman, J. Wang and M. Kaetzel for nCaMBP reagents; D. L. Taylor and J. Montibeller for mCaM; H. Schulman and H. Bito for advice and for comments on the manuscript; and R. Lewis, T. Schwarz and L. Stryer for comments on the manuscript. Supported by grants from the Silvio Conte-NIMH Center for Neuroscience Research, the McKnight Foundation, the Mathers Charitable Trust, and the NIH Medical Scientist Training Program.

Correspondence and requests for materials should be addressed to R.W.T. (e-mail: rwtsien@leland.stanford.edu).

The hyperthermophile chromosomal protein Sac7d sharply kinks DNA

Howard Robinson*, Yi-Gui Gao*, Bradford S. McCrary†, Stephen P. Edmondson†, John W. Shriver† & Andrew H.-J. Wang*

* *Department of Cell and Structural Biology, University of Illinois at Urbana-Champaign, Urbana, Illinois 61801, USA*
† *Department of Medical Biochemistry, School of Medicine, Southern Illinois University, Carbondale, Illinois 62901, USA*

The proteins Sac7d and Sso7d belong to a class of small chromosomal proteins from the hyperthermophilic archaeon *Sulfolobus acidocaldarius* and *S. solfactaricus*, respectively[1,2]. These proteins are extremely stable to heat, acid and chemical agents[3]. Sac7d binds to DNA without any particular sequence preference and thereby increases its melting temperature by ~40 °C (ref. 4). We have now solved and refined the crystal structure of Sac7d in complex with two DNA sequences to high resolution. The structures are examples of a nonspecific DNA-binding protein bound to DNA, and reveal that Sac7d binds in the minor groove, causing a sharp kinking of the DNA helix that is more marked than that induced by any sequence-specific DNA-binding proteins. The kink results from the intercalation of specific hydrophobic side chains of Sac7d into the DNA structure, but without causing any significant distortion of the protein structure relative to the uncomplexed protein in solution.

Sac7d and Sso7d are proteins of relative molecular mass 7,000 (M_r 7K) from *S. acidocaldarius* and *S. solfataricus*, respectively (Fig. 1a). The structures of Sac7d bound to $d(GCGATCGC)_2$ and $d(GTAATTTAC)_2$ have been well refined at 1.6 and 1.9 Å resolution, respectively (Table 1, Fig. 1b). All ϕ/ψ angles in both complexes fall within the acceptable regions. Sac7d binds to the DNA octamer duplex in the minor groove forming a 1:1 complex (Fig. 1c). In the Sac7d–GCGATCGC complex, the protein binds at the C2pG3 step with a sharp kink, covering four base pairs (G1–C16 to A4–T13) and dramatically widens the DNA minor groove. The other end of the